Superhydrophobic Surfaces

Deutsche Ausgabe: DOI: 10.1002/ange.201600224
Internationale Ausgabe: DOI: 10.1002/anie.201600224

Guided Self-Propelled Leaping of Droplets on a Micro-Anisotropic Superhydrophobic Surface

Jie Liu, Haoyuan Guo, Bo Zhang, Shasha Qiao, Mingzhe Shao, Xianren Zhang, Xi-Qiao Feng, Qunyang Li, Yanlin Song, Lei Jiang, and Jianjun Wang**

Abstract: *By introducing anisotropic micropatterns on a superhydrophobic surface, we demonstrate that water microdroplets can coalesce and leap over the surface spontaneously along a prescribed direction. This controlled behavior is attributed to anisotropic liquid–solid adhesion. An analysis relating the preferential leaping probability to the geometrical parameters of the system is presented with consistent experimental results. Surfaces with this rare quality demonstrate many unique characteristics, such as self-powered, and relatively long-distance transport of microdroplets by "relay" coalescence-induced leaping.*

Guided water transport has many applications in microfluidics,[1] printing,[2] oil–water separation,[3] and atmospheric water harvesting.[4] Although successful examples have been demonstrated with external fields,[5] it is often desirable to move water in a preferred direction without any external forces. Ambitions aside, our daily experience tells us that water only flows downward under gravity. The situation changes when water droplets are small in size because surface tension can be utilized to overcome gravity for guided liquid transport. For example, chemical gradients have been used to drive water drops uphill,[6] although with a typically low speed. Assisted by surface energy released during droplet coalescence, condensed microdroplets on solid surfaces with a chemical gradient could move toward a more wettable region with a speed as high as $1.5\,m\,s^{-1}$.[7] Despite these successful examples, self-propelled transport that exploits spatial gradients encounters an intrinsic dilemma: a strong gradient is required to achieve a large driving-force, which inevitably limits the size of the effective working area (usually a few centimeters or less).[5a,7,8] Recently, self-propelled jumping of coalesced microdroplets on super-hydrophobic surfaces[9] suggested a potential means for guided self-propelled transport. A leaping microdroplet only makes intermittent contact with the solid surface, and therefore, a surface with a continuous gradient may not be needed for long-distance transport. Herein, we applied lessons from nature to design of a micro-anisotropic superhydrophobic surface (MATS surface) consisting of periodic isosceles triangle micro-arrays, which enables self-powered and relatively long-distance transport of microdroplets in a guided direction. Figure 1 a shows a series of optical and SEM images of a MATS surface and its microfabricated structure. The MATS surface is completely covered with a layer of nanoporous alumina, which is essential for preserving superhydrophobicity to microdroplets.[10]

The MATS surface exhibits anisotropic liquid–solid adhesion, as implied by the impacting and bouncing behavior of a macroscopic droplet on the surface. Figure 1 b shows a few representative snapshots of the anisotropic bouncing behavior of a macroscopic droplet impacting the MATS surface. Upon touching the MATS surface, the droplet continued to spread nearly symmetrically until a maximum lateral extension (3.15 mm) was reached after 2.60 ms. However, during the bouncing process, the droplet retracted more

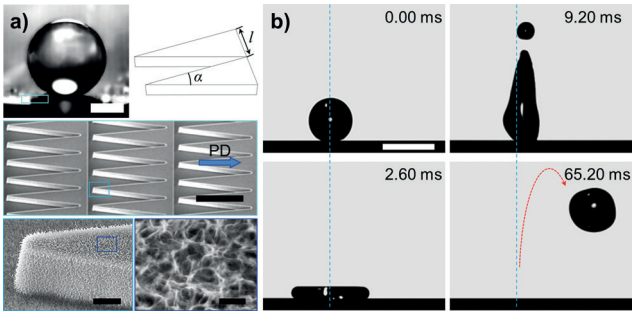

Figure 1. Surface morphology and anisotropic bouncing of a macroscopic drop on a MATS surface. a) Scanning electron microscope (SEM) images of the MATS surface with $l = 10\,\mu m$, $\alpha = 15°$, and a microstructure height of 5 μm. The MATS surface is superhydrophobic with respect to condensed microdroplets, with a contact angle of 170.6°. The microstructure is fully covered with a nanoporous film; the blue arrow shows the positive direction (PD) of guided leaping (Supporting Information, Figure S3). Scale bars (top to bottom): 100 μm, 20 μm, 1 μm, and 100 nm. b) Selected snapshots captured by a high-speed-camera display a water droplet with a radius of 0.89 mm impacting on the MATS surface at a velocity of $0.82\,m\,s^{-1}$, implying that the MATS surface possesses anisotropic liquid–solid adhesion properties. Scale bar: 2 mm.

[*] Dr. J. Liu, Dr. M. Shao, Prof. Y. Song, Prof. L. Jiang, Prof. J. Wang
Key Laboratory of Green Printing, Institute of Chemistry
Chinese Academy of Sciences, Beijing 100190 (China)
E-mail: wangj220@iccas.ac.cn
Dr. H. Guo, Dr. S. Qiao, Prof. X. Feng, Prof. Q. Li
AML and CNMM, Department of Engineering Mechanics, State Key Laboratory of Tribology, Tsinghua University
Beijing 100084 (China)
E-mail: qunyang@tsinghua.edu.cn
Dr. B. Zhang, Prof. X. Zhang
Division of Molecular and Materials Simulation
State Key Laboratory of Organic–Inorganic Composites
Beijing University of Chemical Technology
Beijing 100029 (China)

Supporting information for this article, including experimental details about the fabrication and characterization of materials, is available in the Supporting Information and on the WWW under http://dx.doi.org/10.1002/anie.201600224.

© 2016 Wiley-VCH Verlag GmbH & Co. KGaA, Weinheim

quickly on the left edge than on the right. As shown by the picture taken at 9.20 ms, the different retraction speeds rendered the droplet in an asymmetric shape.[11] The dynamic apparent contact angle on the left side ($\theta_L = 132.0°$) was noticeably larger than that on the right ($\theta_R = 102.1°$; Supporting Information, Figure S1 and S2), suggesting that the equivalent work of adhesion on the left pinning-edge is smaller than that on the right. An asymmetric pinning capability entails a droplet bouncing velocity with a lateral component in the positive direction, as clearly depicted by the snapshot at 65.20 ms of Figure 1b (Supporting Information, Movie S1).

The anisotropic adhesion of the MATS surface also has a profound influence on the coalescence-induced leaping behavior of condensed water microdroplets. Typical side-view snapshots of the guided self-propelled leaping behavior of coalesced water microdroplets on the MATS surface are shown in Figure 2a (top-view images are displayed in the Supporting Information, Figure S4), and are compared side-by-side with typical snapshots taken on an isotropic nanostructured superhydrophobic surface (NASS surface). Consistent with previous reports,[12] the spontaneous jumping direction on the NASS surface was mostly vertical, with a statistically random nature. In sharp contrast, the leaping direction on the MATS surface demonstrated a clear bias in the positive direction. A positive direction is defined by the 2D statistical distribution of the angles of leaping events (Supporting Information, Figure S3). Figure 2b shows a typical guided leaping trajectory of a coalesced droplet on the MATS surface and its velocity variation with time. One can easily see that, as well as the regular vertical jumping velocity

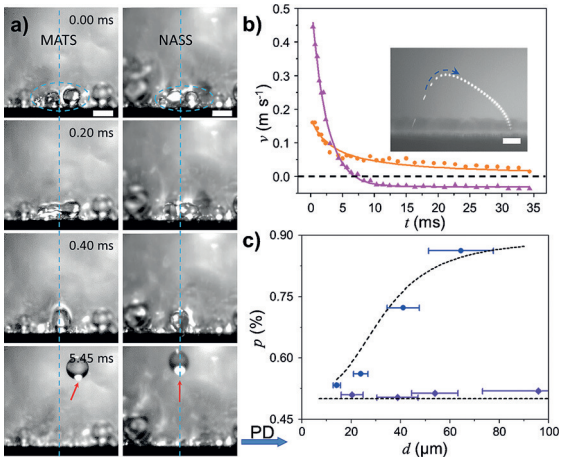

Figure 2. Guided self-propelled leaping. a) Side-view snapshots of a guided self-propelled motion show that the coalesced microdroplet leaps along the positive direction on a MATS surface ($l = 10$ μm, $\alpha = 15°$) but vertically on a NASS surface. Scale bar: 100 μm. b) The MATS surface endows the microdroplet with a non-negligible leaping velocity parallel to the surface (0.17 m s^{-1}) compared to the normal velocity (0.45 m s^{-1}). Experimental velocity normal (—▲—) and parallel (—●—) to the surface. Inset: corresponding trajectory of the leaping microdroplet. Scale bar: 300 μm. c) Preferential leaping probability increases with the diameter of the coalesced microdroplets on the MATS surface ($l = 10$ μm, $\alpha = 15°$, (●)) but remains almost unchanged around 50% on the NASS surface (◆).

(0.45 m s^{-1}), the anisotropic MATS surface provided the microdroplet with a non-negligible initial lateral velocity toward the positive direction (0.17 m s^{-1}). The resistance force of air gives the leaping droplet an asymmetric parabolic shaped trajectory (see detailed analysis in the Supporting Information). Lateral momentum indicates that there must be a net lateral force acting on the coalesced droplet during contact of microdroplets with the MATS surface. To obtain a more exact comparison, we estimated the preferential leaping probability (p) by calculating the ratio of leaping events along the positive direction versus the total jumping events on the MATS and NASS surfaces. Variations of the preferential leaping probability (p) with the diameters of the coalesced microdroplets on both NASS and MATS surfaces are given in Figure 2c. As confirmed by the curves, the jumping direction on the NASS surface is indeed non-biased,[12a] while the jumping direction on the MATS surface exhibits a clear orientation and this preference is more pronounced when the size of the coalesced water droplet is larger. For example, Figure 2c reveals that 54% of the coalesced microdroplets leaped along the positive direction when their size was around 14 ± 2 μm, but the ratio increased to 86% when the droplet size was around 63 ± 11 μm. It is worth mentioning that a certain number of smaller droplets initially leaped in the negative direction, but subsequently reversed direction and eventually leaped in the positive direction after a series of coalescences (Supporting Information, Figure S5). This is another unique feature of our MATS system.

A representative coalescence and leaping event of two condensed water droplets on the MATS surface was monitored with a high-speed-camera, as shown in Figure 3a. The coalescence started with formation of a liquid bridge between two adjoining droplets, followed by rapid expansion of the connecting bridge. At a certain moment ($t = 1.61$ ms in our example) the liquid bridge grew large enough to impact on the substrate surface and we noticed that there was no visible asymmetric deformation until liquid–solid contact was maximized. Subsequently, the coalesced microdroplet bounced up and the solid–liquid interface began to shrink.[9a,13] As can be seen from a snapshot ($t = 1.82$ ms, Figure 3a), during the retracting process the morphology of the coalesced microdroplet became noticeably asymmetric. The dynamic contact angle on the right retracting-edge was smaller than that on the left, therefore the three-phase contact-line (TCL) was better pinned and moved more slowly on the right edge. This asymmetric pinning process continued until the coalesced microdroplet eventually leaped in the positive direction on the MATS surface, as shown by the image taken at $t =$ 23.63 ms (Supporting Information, Movie S2). Based on the details shown in Figure 3a, Figure 3b illustrates the asymmetric retraction process. The smaller dynamic contact angle on the right ($\theta_L > \theta_R$), and the slower retraction speed of the right TCL, suggest that the apparent pinning force ($F_{pinning}$) on the right TCL is larger than that on the left ($F_{pinning,Right} > F_{pinning,Left}$), which is also verified by a water droplet friction experiment on the MATS surface (Supporting Information, Figure S6). This asymmetric and unbalanced pinning force results in a net lateral momentum of the coalesced micro-

© 2016 Wiley-VCH Verlag GmbH & Co. KGaA, Weinheim

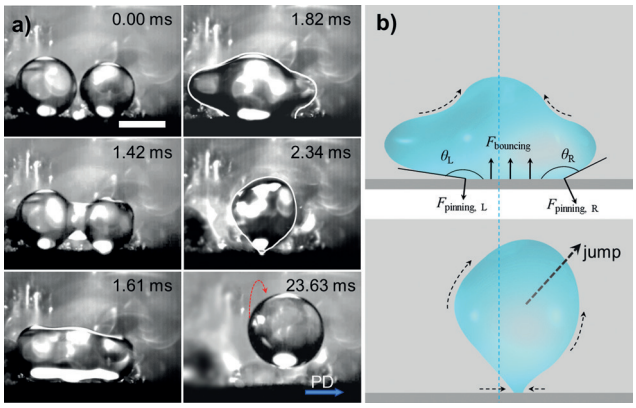

Figure 3. Driving-force for guided self-propelled microdroplet leaping. a) High-speed-camera sequential images of a representative guided self-propelled leaping event on the MATS surface ($l = 10$ μm, $\alpha = 15°$). A liquid bridge forms between two coalescing microdroplets at 1.42 ms, and subsequently grows and impacts on the substrate at 1.61 ms. During the retraction process, the coalesced microdroplet displays an asymmetric shape, presenting a contact angle at the left pinning-edge that is larger than that at the right (see image taken at 1.82 ms). The coalesced microdroplet finally leaps along the positive direction (see image taken at 23.63 ms). Scale bar: 200 μm. b) Illustration of the forces exerted on the retracting microdroplet. The coalesced microdroplet experiences an upward bouncing force ($F_{bouncing}$) because of the impact of the liquid bridge on the MATS surface. Recession of the TCL at the left edge is faster than that at the right, and the mass center of the microdroplet moves up and to the right (lower graphic).

droplet during the leaping process, which is analogous to the bouncing process of the macrodroplet impacting on the MATS surface, as shown in Figure 1c. According to an early study,[14] the apparent work of adhesion is related to the receding contact angle by

$$W_{ad,ap} = \gamma_{L\text{-}V}(1 + \cos\theta_{rec}) \quad (1)$$

where $\gamma_{L\text{-}V}$ is the interfacial energy of the liquid–vapor interface, and θ_{rec} is the receding contact angle of the microdroplet. Based on this estimation, the apparent work of adhesion on the left edge is smaller than that on the right, $W_{ad,L} < W_{ad,R}$. Although, strictly speaking, Equation (1) holds only for an equilibrated process, it still gives a reasonable and qualitative comparison of the strength of liquid–solid adhesion.[11a]

Based on the mechanism proposed above, guided leaping of the coalesced microdroplets depends on the location of the coalescence and the morphology of the MATS surface. If we further assume that the coalescence sites are uniformly random on the MATS surface, then the probability (p) with which a coalesced droplet will leap along the positive direction is a function of the geometric parameters of the MATS surface and the droplet size:

$$p = \mathrm{fn}\left(\alpha, \frac{d}{l}, \frac{\sqrt{\gamma_{int}/\rho g}}{l}\right) \quad (2)$$

where α and l are the vertex angle and the bottom edge length of the micropattern, respectively, d is the diameter of the coalesced microdroplet, γ_{int} is the intrinsic liquid–solid adhesion, ρ is the density of water, and g is the gravitational acceleration. The relative size of coalescing droplets and the height of the microstructure would also affect leaping, but herein we focus on the effect of d/l and α by carrying out the experiments in a closed chamber with a relative humidity of 100%, and by fixing the height to 5 μm (see the analysis in the Supporting Information).

To identify the trend predicted by expression (2), we systematically varied the geometry of the micropattern (namely the values of l and α) and recorded the corresponding probability of positive-leaping events. As shown in Figure 4, variation of p seems to scale with d/l when α is fixed at 15° on a master curve for all MATS samples with different geometries. The probability (p) increases with increasing d/l, and decreases when α increases from 15° to 60° (leaping direction is nearly random when $\alpha = 60°$ ($p = 0.5$); inset of Figure 4). These experimental results suggest that, for the length scale explored in our MATS surface experiments, the dependence of p can be further reduced.

$$p = \mathrm{fn}\left(\alpha, \frac{d}{l}\right) \quad (3)$$

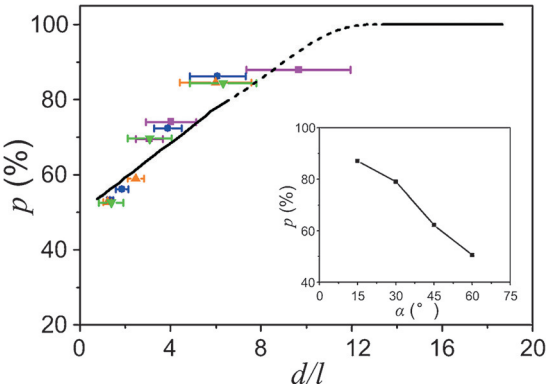

Figure 4. Dependence of leaping statistics on geometric parameters of the MATS surface. Variations of probability of positive leaping events versus the normalized size of the coalesced droplets on four different MATS samples ($l = 5$ μm (■), 10 μm (●), 15 μm (▲), 20 μm (▼), at $\alpha = 15°$); theory (——); inset: variation of p versus the vertex angle for relatively large droplets ($d/l \approx 7$).

An analysis was thus proposed based on the magnitude of the ratio between the size of the solid–liquid contact region with respect to the dimension of the micropatttern (Supporting Information, Figure S8). A prediction of p versus d/l was performed for MATS samples with typical parameters over two liquid–solid contact size regimes, and is shown in Figure 4 as two solid curves. In the moderate contact size range, a smooth dashed line was interpolated to aid visual interpretation of the trend. Despite this simplification in the analysis, the prediction is reasonably consistent with the experimental data.

A time-lapse image (with a long exposure time 0.18 s) of leaping microdroplets with relatively large sizes is shown in

 © 2016 Wiley-VCH Verlag GmbH & Co. KGaA, Weinheim

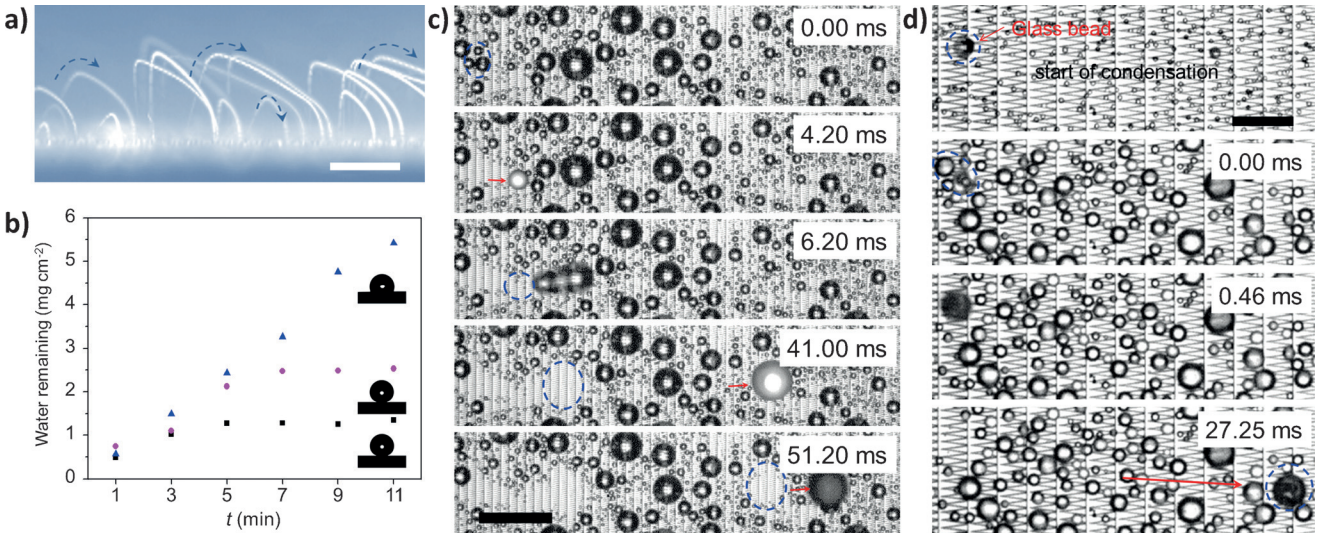

Figure 5. a) Time-lapse ($\Delta t = 0.18$ s) image of leaping microdroplets on the MATS surface showing guided leaping in the positive direction. Scale bar: 100 μm. b) Mass transfer and high water removal capability on the MATS surface ($l = 10$ μm, $\alpha = 15°$). Mass of remaining droplets on a flat aluminum surface modified with FAS-17 (▲). Mass of remaining droplets on the MATS surface ($l = 10$ μm, ■, $\alpha = 15°$) and NASS surface (●). The amount of water remaining on the flat aluminum surface grows linearly with time, but is almost unchanged on the NASS and MATS surfaces at a condensing time of 7 min (the water vapor supersaturation ratio is 2.18). The amount of water remaining on the MATS surface is half of that on the NASS surface and about one quarter of that on the flat hydrophobic surface at 11 min. c) As the coalesced microdroplet has a lateral momentum, a "relay" of coalescence events happens easily, facilitating long distance transport of microdroplets. Scale bar: 0.5 mm. d) The microdroplet works as a self-sustained microcarrier. When the microdroplet coalesces on the MATS surface with a glass bead with a diameter of about 30 μm (indicated at 0.00 ms), the bead moves directionally along the surface, as shown in the picture taken at 27.25 ms. Scale bar: 100 μm.

Figure 5a, which clearly demonstrates the reproducibility of leaping direction of coalesced microdroplets (Supporting Information, Movie S3). Surfaces able to guide the self-propelled leaping of droplets demonstrate a greatly enhanced mass transfer performance.[15] As shown in Figure 5b, the amount of water remaining on the MATS surface is half of that on the NASS surface, and is about one quarter of that on the flat hydrophobic surface 11 min after condensation starts. Additionally, efficient self-powered, and relatively long-distance transport could be achieved on the MATS surface by "relay" coalescence-induced leaping (Figure 5c; Supporting Information, Movie S4). The transport distance was up to two orders of magnitude greater than the diameter of the initial coalesced microdroplet. For this reason the MATS surface exhibits a better water removing performance than the NASS surface. Moreover, on the basis of guided self-propelled leaping, the droplet could work as an effective self-sustained microcarrier (see Figure 5d, where a glass bead is carried along the positive direction).

In conclusion, a micro-anisotropic superhydrophobic surface (MATS surface) was designed using the work of adhesion as a steering force for leaping microdroplets. For the first time, leaping of droplets in a guided lateral direction on superhydrophobic surfaces can be achieved without any external forces. Described herein, surfaces with this rare quality demonstrate unique properties; including self-powered and relatively long-distance transport by "relay" coalescence-induced leaping and effective self-sustained microcarrier, as well as greatly enhanced heat, mass and energy transfer performance (Supporting Information, Figure S9).[15]

Acknowledgements

We gratefully acknowledge financial support from the 973 Program 2013CB933000, the National Natural Science Foundation of China (51436004, 51173196, 21421061, 11432008, and 11422218).

Keywords: anisotropy · microdroplets · guided propulsion · self-propelled movement · superhydrophobicity

How to cite: *Angew. Chem. Int. Ed.* **2016**, *55*, 4265–4269
Angew. Chem. **2016**, *128*, 4337–4341

[1] a) G. Lagubeau, M. Le Merrer, C. Clanet, D. Quéré, *Nat. Phys.* **2011**, *7*, 395–398; b) G. M. Whitesides, *Nature* **2006**, *442*, 368–373; c) T. M. Schutzius, S. Jung, T. Maitra, G. Graeber, M. Kohme, D. Poulikakos, *Nature* **2015**, *527*, 82–85.
[2] J. Z. Wang, Z. H. Zheng, H. W. Li, W. T. S. Huck, H. Sirringhaus, *Nat. Mater.* **2004**, *3*, 171–176.
[3] K. Li, J. Ju, Z. X. Xue, J. Ma, L. Feng, S. Gao, L. Jiang, *Nat. Commun.* **2013**, *4*, 2276.
[4] a) L. Jiang, J. Ju, H. Bai, Y. Zheng, T. Zhao, R. Fang, *Nat. Commun.* **2012**, *3*, 1247; b) Y. Zheng, H. Bai, Z. Huang, X. Tian, F. Q. Nie, Y. Zhao, J. Zhai, L. Jiang, *Nature* **2010**, *463*, 640–643.
[5] a) N. A. Malvadkar, M. J. Hancock, K. Sekeroglu, W. J. Dressick, M. C. Demirel, *Nat. Mater.* **2010**, *9*, 1023–1028; b) K. Ichimura, S.-K. Oh, M. Nakagawa, *Science* **2000**, *288*, 1624–1626.
[6] M. K. Chaudhury, G. M. Whitesides, *Science* **1992**, *256*, 1539–1541.
[7] S. Daniel, M. K. Chaudhury, J. C. Chen, *Science* **2001**, *291*, 633–636.
[8] a) T. Sanchez, D. T. Chen, S. J. DeCamp, M. Heymann, Z. Dogic, *Nature* **2012**, *491*, 431–434; b) H. Linke, B. J. Aleman, L. D. Melling, M. J. Taormina, M. J. Francis, C. C. Dow-Hygelund, V.

 © 2016 Wiley-VCH Verlag GmbH & Co. KGaA, Weinheim

Narayanan, R. P. Taylor, A. Stout, *Phys. Rev. Lett.* **2006**, *96*, 154502.
[9] a) J. B. Boreyko, C.-H. Chen, *Phys. Rev. Lett.* **2009**, *103*, 184501; b) Y. Luo, J. Li, J. Zhu, Y. Zhao, X. Gao, *Angew. Chem. Int. Ed.* **2015**, *54*, 4876 – 4879; *Angew. Chem.* **2015**, *127*, 4958 – 4961.
[10] a) A. Lafuma, D. Quere, *Nat. Mater.* **2003**, *2*, 457 – 460; b) T. Verho, J. T. Korhonen, L. Sainiemi, V. Jokinen, C. Bower, K. Franze, S. Franssila, P. Andrew, O. Ikkala, R. H. Ras, *Proc. Natl. Acad. Sci. USA* **2012**, *109*, 10210 – 10213; c) G. Azimi, R. Dhiman, H.-M. Kwon, A. T. Paxson, K. K. Varanasi, *Nat. Mater.* **2013**, *12*, 315 – 320; d) T. Zhang, J. Wang, L. Chen, J. Zhai, Y. Song, L. Jiang, *Angew. Chem. Int. Ed.* **2011**, *50*, 5311 – 5314; *Angew. Chem.* **2011**, *123*, 5423 – 5426.
[11] a) B. A. Malouin, Jr., N. A. Koratkar, A. H. Hirsa, Z. Wang, *Appl. Phys. Lett.* **2010**, *96*, 234103; b) M. Reyssat, A. Pépin, F. Marty, Y. Chen, D. Quéré, *Europhys. Lett.* **2006**, *74*, 306 – 312; c) J. C. Bird, R. Dhiman, H. M. Kwon, K. K. Varanasi, *Nature* **2013**, *503*, 385 – 388; d) A. Gauthier, S. Symon, C. Clanet, D. Quéré, *Nat. Commun.* **2015**, *6*, 8001; e) Y. Liu, M. Andrew, J. Li, J. M. Yeomans, Z. Wang, *Nat. Commun.* **2015**, *6*, 10034.
[12] a) X. Qu, J. B. Boreyko, F. Liu, R. L. Agapov, N. V. Lavrik, S. T. Retterer, J. J. Feng, C. P. Collier, C.-H. Chen, *Appl. Phys. Lett.* **2015**, *106*, 221601; b) F. Liu, G. Ghigliotti, J. J. Feng, C. Chen, *J. Fluid Mech.* **2014**, *752*, 22 – 38.
[13] F. Liu, G. Ghigliotti, J. J. Feng, C.-H. Chen, *J. Fluid Mech.* **2014**, *752*, 39 – 65.
[14] L. Gao, T. J. McCarthy, *Langmuir* **2009**, *25*, 14105 – 14115.
[15] a) Y. Hou, M. Yu, X. Chen, Z. Wang, S. Yao, *ACS Nano* **2015**, *9*, 71 – 81; b) N. Miljkovic, D. J. Preston, R. Enright, E. N. Wang, *ACS Nano* **2013**, *7*, 11043 – 11054.

Received: January 8, 2016
Published online: March 1, 2016

 © 2016 Wiley-VCH Verlag GmbH & Co. KGaA, Weinheim